Title

Hypertrophic and fibrotic human PKD hearts are associated with macrophage infiltration and abnormal TGF-β1 signaling

Journal

Cell and Tissue Research, 391(1)

ISSN

0302-766X

Authors

Amirrad, Farideh
Fishbein, Gregory A
Edwards, Robert A
et al.

Publication Date

2023

DOI

10.1007/s00441-022-03704-y

Peer reviewed

HHS Public Access

Author manuscript

Cell Tissue Res. Author manuscript; available in PMC 2023 July 01.

Published in final edited form as:

Cell Tissue Res. 2023 January ; 391(1): 189–203. doi:10.1007/s00441-022-03704-y.

Hypertrophic and fibrotic human PKD hearts are associated with macrophage infiltration and abnormal TGF-β_1 signaling

Farideh Amirrad[1,2], **Gregory A. Fishbein**[3], **Robert A. Edwards**[4], **Surya M. Nauli**[1,2]

[1]Department of Biomedical and Pharmaceutical Sciences, Chapman University, 9401 Jeronimo Road, Irvine, CA 92618-1908, USA

[2]Department of Medicine, University of California Irvine, Orange, CA 92868, USA

[3]Department of Anatomic Pathology, David Geffen School of Medicine at UCLA, Los Angeles, CA 90095, USA

[4]Department of Pathology and Lab Medicine, University of California Irvine Orange CA 92868 USA

Abstract

Autosomal dominant polycystic kidney disease (PKD) is a hereditary kidney disorder which can affect cardiovascular system. Cardiac hypertrophy and cardiomyopathy in PKD have been reported by echocardiography analyses, but histopathology analyses of human PKD hearts have never been examined. The current studies evaluated human heart tissues from five subjects without PKD (non-PKD) and five subjects with PKD. Our histopathology data of human PKD hearts showed an increased extracellular matrix associated with cardiac hypertrophy and fibrosis. Hypertrophy- and fibrosis-associated pathways involving abnormal cardiac structure were next analyzed. We found that human PKD myocardium was infiltrated by inflammatory macrophage M1 and M2; expression of transforming growth factor (TGF-β_1 and its receptor were upregulated with overexpression of pSmad3 and β-catenin. Because patients with PKD have an abnormal kidney function that could potentially affect heart structure, we used a heart-specific PKD mouse model to validate that cardiac hypertrophy and fibrosis were independent from polycystic kidney. In summary, our data show that hearts from human PKD were characterized by hypertrophy, interstitial fibrosis, perivascular fibrosis, and conduction system fibrosis with upregulated TGF-β_1

Surya M. Nauli, nauli@chapman.edu; snauli@uci.edu.

Author contribution FA collected and analyzed data, drafted the manuscript, oversaw the experimental progress, and served as a double-blind operator. GAF and RAE collected and assisted in procuring and processing human tissue samples. SMN drafted the manuscript and served as a double-blind operator. All authors participated in finalizing the manuscript.

Supplementary Information The online version contains supplementary material available at https://doi.org/10.1007/s00441-022-03704-y.

Availability of data and materials The data that support the findings of this study are available from the corresponding author on reasonable request. Some data and samples may not be made available because of privacy or ethical restrictions.

Ethics approval and consent to participate The human-subjects research project was approved by and per accordance with the Chapman University Institutional Review Board (IRB# 1415H040 and FWA#00011020). The approval for tissue procurement was extended to each respective site identified in our IRB application. All retrospective samples from deceased subjects had been previously de-identified by the Department of Pathology and Laboratory Medicine at the UC Los Angeles and UC Irvine.

Consent for publication All authors consent these studies for publication.

Conflict of interest The authors declare no competing interests.

and its receptor. We suggest that such structural abnormalities may predispose to systolic and diastolic cardiac dysfunction in the PKD myocardium.

Keywords

Kidney disorder; Fibrosis; Hypertrophy

Introduction

Autosomal dominant polycystic kidney disease (PKD) is a multisystem disorder characterized by the formation of many fluid-filled cysts in the kidneys, pancreas, liver, and cardiovascular complications (Kim et al. 2000). Mutations in *PKD1* and *PKD2* genes contribute to approximately 85% and 15% cases, respectively, and they are the most common genetic kidney disorder that causes end-stage renal failure in adulthood (Cornec-Le Gall et al. 2019; Kurschat et al. 2014).

Cardiovascular manifestations in PKD patients include hypertension, left ventricular hypertrophy (LVH) (Chapman et al. 1997), valvular heart disease (Leier et al. 1984), intracranial and extracranial aneurysms (Pirson et al. 2002), coronary artery dissection (Cornec-Le Gall et al. 2019), and atrial fibrillation (Yu et al. 2016). In some cases, mutations in PKD genes are also associated with isolated cardiomyopathy before any renal abnormality is detected (Chebib et al. 2017; Morita 2019). This suggests that a molecular abnormality causing PKD can directly cause cardiomyopathy independent of hypertension or renal failure. Thus, cardiomyopathy could be a cardiac manifestation of systemic PKD syndrome.

LVH is a powerful independent risk factor for cardiovascular morbidity and mortality. PKD patients have a high prevalence of LVH (Chapman et al. 1997; Schrier 2009), often associated with a poor prognosis (Gosse 2005). The LVH is associated with cardiac fibrosis in PKD patients as analyzed through echocardiography (Suwa et al. 2019). Although the histopathology of human PKD hearts has never been directly studied, animal models have shown LVH associated with cardiac fibrosis (Amirrad et al. 2021; Aranguiz et al. 2021; Balbo et al. 2016). Cardiac fibrosis is characterized by the accumulation of extracellular matrix proteins in the cardiac interstitium, and it contributes to systolic and diastolic dysfunction in many cardiac pathophysiologic conditions, including PKD mice (Amirrad et al. 2021; Klein et al. 2005).

Many studies have shown that over-expression of Wnt/β-catenin is necessary to induce hypertrophy in cultured adult cardiomyocytes and animal models (Chen et al. 2006; Haq et al. 2003). TGF-β_1, a key fibrogenic mediator involved in the cardiac fibrotic responses, can also regulate the Wnt/β-catenin pathway (Kong et al. 2014; Lijnen and Petrov 2002; Riemann et al. 1994). TGF-β_1 is thus markedly induced in hypertrophied myocardium and has an important role in regulating cardiomyocyte hypertrophy (Azhar et al. 2003; Hanna and Frangogiannis 2019; Villarreal and Dillmann 1992). The canonical pathway of TGF-β_1 signaling can also regulate Smad2/3 phosphorylation, which subsequently translocates to the nucleus. In the nucleus, it functions as a transcription factor and activates numerous pro-fibrotic genes (Bujak and Frangogiannis 2007; Bujak et al. 2007).

Since there is currently no study on histopathology analysis of human PKD hearts, our current studies examined changes in cardiac structures and their associated pathways including the roles of TGF-β_1, p-Smad3, and β-catenin in human PKD hearts. Together with the premises from our prior animal studies that myocardial dysfunction in PKD is caused by structural abnormalities (Amirrad et al. 2021), we hypothesize that hearts from PKD patients develop fibrosis and hypertrophy via a dysregulated signaling pathway involving TGF-β_1, p-Smad3, and β-catenin.

Materials and methods

Throughout our studies, we used fixed heart tissues from deceased subjects without (non-PKD) and with (PKD) polycystic kidney disease. Our subjects had been previously de-identified, and samples from the subjects were obtained from the Department of Pathology and Laboratory Medicine at the UC Los Angeles and UC Irvine. The human-subjects research project was approved by and per accordance with the Chapman University Institutional Review Board. The approval for tissue procurement was extended to each respective site identified in our IRB application. Five PKD subjects were first identified for their sexes; this information was then used to select non-PKD subjects as controls (Table 1).

Immunofluorescence studies

For evaluation of protein localization and expression, paraffin section tissues were deparaffinized and dehydrated. Heat-induced epitope retrieval was performed using a pressure cooker and sodium citrate buffer (10 mM sodium citrate, 0.05% Tween-20, pH 6.0). Slides were placed into the 98 °C antigen retrieval buffer in the pressure cooker for 20 min and then removed from the pressure cooker and cooled to room temperature for 30 min. For permeabilization, slides were incubated with permeabilization buffer (0.3% Triton-X in PBS) for 10 min and then blocked with PBS-T (PBS + 0.1% Tween-20) solution containing 5% bovine serum albumin (BSA) and 0.1% Triton-X. Subsequently, the slides were incubated in specific primary antibodies to detect target proteins. All washing steps were done three times with PBS-T.

For cell membrane staining and cell size measurement, tissue slides were incubated with FITC-labeled wheat germ agglutinin (WGA) (1:1000; Cat# FL-1021; Vectorlabs) for 20 min. To study fibrotic pathways in human heart tissue, human heart slides were incubated with anti-pSMAD3 (1:1000; Cat# sc-517575; Santa Cruz, Inc.), anti-β-catenin (1:50; Cat# sc-133240; Santa Cruz, Inc.), anti-α-actin (1:100; Cat# sc-32251; Santa Cruz, Inc.), anti-COL1A1 (1:100; Cat# sc-293182; Santa Cruz, Inc.), and anti-YAP1 (1:100; Cat# sc-101199; Santa Cruz, Inc.) antibodies overnight at 4 °C in a humidified chamber followed with AlexaFluor-488 secondary goat anti-mouse antibody (1:1000; Cat# ab150113; Abcam, Inc.). For evaluation of macrophage infiltration, slides were incubated overnight at 4 °C in a humidified chamber with anti-NOS2 (1:50; Cat# sc-7271; Santa Cruz, Inc.) and anti-CD-86 (1:50; Cat# sc-52448; Santa Cruz, Inc.) antibodies for macrophage M1 detection, or anti-CD163 antibody (1:50; sc-20066; Santa Cruz, Inc.) and anti-CD-206 (1:100; Cat# ab91992; Signaling, Inc.) antibodies for macrophage M2 detection, followed with AlexaFluor-594 goat anti-mouse fluorescence (1:500; Cat# 8890; Signaling, Inc.), AlexaFluor-488 goat

anti-rabbit fluorescence (1:500; Cat# 4412; Signaling, Inc.), or AlexaFluor-488 goat anti-rat fluorescence secondary antibodies (1:500; Cat# ab6840; Abcam, Inc.). 4′,6-diamidino-2-phenylindole (DAPI) was used as a nuclear binding dye for all slides.

Immunohistology staining

For evaluation of TGF-β_1 and its receptor expression, tissue slides underwent deparaffinization and dehydration, followed with epitope retrieval. After permeabilization, endogenous peroxidase activity was blocked with 3% hydrogen peroxide for 10 min, and unspecific bindings were blocked with animal-free blocking solution (Cat# 15,019; Cell Signaling, Inc.). Slides were incubated at 4 °C overnight with primary mouse monoclonal anti-TGF-β_1 (1:50; Cat# sc-130348; Santa Cruz, Inc.) or rabbit polyclonal anti-TGF-β_1 receptor (1:100; Cat# ab235178; Abcam, Inc.). Slides were then washed and incubated in Signal Stain Boost Detection Reagent (HRP mouse; Cat# 8125; or HRP Rabbit; Cat# 8114; Cell Signaling, Inc.) for 30 min at room temperature and incubated in Signal Stain DAB (Cat# 8059; Cell Signaling, Inc.) for 3 min. Finally, hematoxylin (Cat# 14,166; Cell Signaling, Inc.) was used for nuclear staining and slides were mounted with cover-slips. All washing steps were done three times with PBS-T.

Animal mouse model

In our study, mouse model was used to examine the structural changes and fibrosis in the heart and kidney samples. The study was approved by the Chapman University Institutional Animal Care and Use Committee (IACUC# 2020–1132 and PHS# D17-00,960). Heart-specific transgenic mice were used; *Myh6•Pkd2*$^{wt/wt}$ was used as wild-type (WT; control), and *Myh6•Pkd2*$^{flox/flox}$ was used as a *Pkd2* or PKD. Heart and kidney fibroses were evaluated at 6 months of age. Male and female mice were used in the study, and gender was discovered to be an independent variable to heart and kidney structural changes.

Data and statistical analysis

Fluorescent images were captured with a Nikon A1R+ confocal microscope. Immunohistochemistry images were collected with Keyence BZ-X710 or Nikon Eclipse Ti microscope. Image analyses were performed using Nikon NIS-Element for Advanced Research software (version 4.51). This software was also used for image segmentation, 3D-object reconstruction, and automatic object recognition. Binary masking was used to calculate cell number, cell size, nuclear size, fibrosis, and image intensity for protein expression and localization. To resolve fine details of the images and to maintain consistency in measurements, images were kept at a 1392 × 1040 imaging array. Image scale bar is shown in each group of the images when images were processed at the same time. Otherwise, each figure has its own scale bar.

GraphPad Prism for macOS (version 9.3) was used in the statistical analysis. In all analyses, comparison of unpaired datasets between non-PKD and PKD was made with two-tailed nonparametric Student *t*-test assuming no Gaussian distribution. For each group, we have five independent samples ($N = 5$). For each sample, an average of 6–100 measurements was taken. Distribution analyses were also performed and visualized on all data sets from every sample to confirm normal distribution or heterogeneous variance. All quantifiable data are

reported as the mean ± SEM. $P < 0.05$ was considered significant in our studies. A more precise p value was reported separately in the graphs.

Results

To identify any structural changes in the polycystic kidney disease (PKD) hearts, we used fixed heart tissues from five deceased male donors without PKD (non-PKD) and five deceased male PKD donors. The average age of non-PKD subjects was 63.6 years, and PKD was 58.4 years. The gross descriptions from the pathology reports dictated that these subjects had cardiac hypertrophy. Two of the five PKD patients had medical history of hypertension. Medical history showed the evidence of one pulmonary hypertension (PH) and two coronary artery disease (CAD) in non-PKD subjects.

Human PKD hearts were characterized by hypertrophy and fibrosis

Left ventricular tissues were analyzed in both non-PKD and PKD hearts. WGA and DAPI staining demonstrated cardiomyocyte (Fig. 1a-c) and nuclear (Fig. 1d-f) hypertrophy in PKD hearts, compared to non-PKD hearts (Fig. 1g, h). Data distribution for each sample was tabulated (Fig. 1i-l). Masson trichrome staining also confirmed the left ventricular hypertrophy in PKD based on the myocyte size (Fig. 2a, b) and enlarged nucleus (Fig. 2c, d). Data distribution for each sample was averaged (Fig. 2e, f) and tabulated (Fig. 2g-j).

Increased extracellular matrix (ECM), disorganized myocardial structure, and myofiber disarray in some regions of myocardium were detected in PKD and not in non-PKD hearts (Fig. 3a, b; Supp Fig. 1a, b). For evaluation of tissue fibrosis, we used Masson trichrome staining. Cardiac fibrosis was quantified by calculating the percentage of cardiac tissue occupied by collagen fibers (blue color) in different heart sections. Compared to non-PKD, PKD LV showed higher indices of fibrosis (Supp Fig. 1c, d), including reactive interstitial fibrosis (Fig. 3c, d), perivascular fibrosis (Fig. 3c, d), and His-Purkinje fiber fibrosis (Fig. 3e, f). Data distribution for each sample was averaged (Fig. 3g-i) and tabulated (Fig. 3j-o). It is generally known that increases in myocyte size, nucleus size, ECM, and interstitial fibrosis provide a strong indicator for cardiac hypertrophy in human hearts (Frangogiannis 2019). This suggested that hypertrophied PKD hearts were characterized by fibrosis.

Fibrotic TGF-β_1/pSmad3/β-catenin pathway was activated in human PKD hearts

To examine fibrotic pathway activation, immunohistochemistry was performed to evaluate TGF-β_1 and TGF-β_1 receptor expressions. Expression level was determined by chromogenic dark-brown color produced by immunoperoxidase reaction. For expression quantification, the percentage of cardiac tissue stained by the peroxidase reaction (dark-brown color) was calculated in different heart sections. Expressions of both TGF-β_1 (Fig. 4a, b) and TGF-β_1 receptor (Fig. 4c, d) were significantly higher in PKD compared to non-PKD hearts (Fig. 4e, f). Data distribution for each sample was tabulated (Fig. 4g-j).

To analyze downstream effects of TGF-β_1, we quantified nuclear translocations of pSmad3 and β-catenin with immunofluorescent microscopy. For each individual myocyte, nuclear and cytosolic fractions were carefully discriminated by a confocal microscope for pSmad3 (Fig. 5a-f) and β-catenin (Fig. 5g-l). The total, cytosolic, and nuclear pSmad3 were

significantly greater in PKD than non-PKD myocytes (Fig. 5m). Likewise, the total and cytosolic β-catenin expression levels were significantly higher in PKD than non-PKD myocytes (Fig. 5n). Data distributions of pSmad3 and β-catenin for each sample were tabulated (Supp Fig. 2). The data suggested that both fibrotic pathways of pSmad3 and β-catenin were activated in human PKD hearts, presumably through activation of TGF-β_1 receptor.

Additional analyses were performed to examine levels of myofibroblast, collagen I, and YAP (Yes-associated protein-1) expression (Supp Fig. 3). We confirmed that myofibroblasts were increased in LV of PKD with higher deposition of collagen I and YAP expression.

Human PKD hearts were characterized by macrophage infiltration

We previously showed that the initial fibrotic signaling could potentially derive from macrophages (Amirrad et al. 2021), which are known as a local source for TGF-β_1 (Wang et al. 2021). Judging from our histology findings, human PKD hearts had an increase in ECM and fibrosis, indicating potential inflammation in the myocardium. We thus investigated the potential role of macrophage M1 and M2 in fibrosis. We used CD86 and eNOs as M1 markers (Fig. 6a-f); CD206 and CD163 were used as M2 markers (Fig. 6g-l). The immunofluorescence analyses revealed that compared to non-PKD, human PKD hearts were significantly infiltrated by both macrophages M1 and M2 (Fig. 6m). Data distribution for each macrophage marker was tabulated to show the count of the occurrences of values within a particular sample (Supp Fig. 4). Together, our data suggested that human PKD hearts were grossly infiltrated by macrophage M1 and M2.

Heart-specific PKD mouse model was characterized with cardiac hypertrophy and fibrosis with normal kidney structure

To rule out a potential effect of chronic kidney disease (cystic kidneys) on hearts, we utilized a transgenic PKD mouse model to target heart-specific knockout of *Pkd2* gene using Myh6 mice. The transgenic PKD mice had a normal kidney structure (Supp Fig. 5a) with no apparent changes in the renal tubules (Supp Fig. 5b). As expected, the transgenic PKD mice showed cardiac hypertrophy (Supp Fig. 5c) (Amirrad et al. 2021). We observed not only left ventricle hypertrophy but also right ventricle hypertrophy in PKD heart-specific model, indicating that cardiac abnormality in PKD was independent from cystic kidneys. Further analysis also indicated an increase in interstitial cardiac fibrosis in PKD mouse heart compared to wild-type (Supp Fig. 5d).

Discussion

Autosomal dominant polycystic kidney disease (PKD) is known to have kidney fibrosis (Norman 2011) and cardiac fibrosis in animal models (Pala et al. 2019a, b). However, the histopathology analysis of the heart tissues from human PKD patients has never been reported, despite the fact that cardiovascular complications are the most common leading cause of death in these patients (Fick et al. 1995; Iglesias et al. 1983). For the past decades, we primarily extrapolated our knowledge from human kidney to heart or from mouse models to PKD patients. As a result, we tended to overlook that fibrosis is an organ- and

disease-specific process (Zeisberg and Kalluri 2013). Therefore, our current studies provided significant values to evaluate structural changes and its underlying mechanism in the human PKD heart tissues.

The challenges in using human tissues are primarily due to the access to the autopsy samples from the PKD patients. In these studies, we were able to compare relatively small sample size from the same sex of non-PKD and PKD patients ($N = 5$ each). Given the sample size and inaccessibility to the fresh samples, our studies had several limitations that constrained us from doing more elaborated mechanistic intervention. Regardless, we presented data distribution for each individual sample to demonstrate data variability in all our measurements.

Another limitation of our current studies was that we could not exclude the roles of renal function between non-PKD and PKD groups. At least in different mouse models, the vascular endothelial-specific PKD knockout also causes cardiac hypertrophy and fibrosis (Pala et al. 2019a, b). Interestingly, our previous study using the myocardial-specific PKD knockout mice also shows heart-specific effects, including cardiac hypertrophy and fibrosis (Amirrad et al. 2021). We therefore believe that human PKD is a complex multi-organ disease; the complexity of cardiac functions depends on the heart itself (Amirrad et al. 2021) and its physiological interactions with the blood vessels (Amirrad et al. 2021) and kidney cyst expansion (Chapman et al. 1990; Nauli 2011).

In our current mouse studies, we utilized *Pkd2*$^{flox/flox}$ mice with cardiac-specific mutation (*MyH6Cre*). Because MyH6Cre is known to be highly efficient (Huang et al. 2021), our mouse model carried mutations in both *Pkd2* allele. Although we were not able to perform mutation analysis in the PKD human samples, it is fair to assume that our PKD donors had inherited a germline mutation from their parents. It is our assumption that, like the “second hit” occurring in the kidneys of the PKD patients (Dong et al. 2021; Ong et al. 1999), a potential “second hit” could have also occurred in different organs including the hearts. Consistent with this assumption, many PKD patients are also characterized by cystic livers (Cnossen and Drenth 2014), cardiomyopathies (Chebib et al. 2017), and others. Given a potential “second hit” in the heart, heart disease in PKD does not necessarily have to be associated with hypertension as indicated in our PKD patients.

Our current study also showed left ventricular hypertrophy (LVH) and interstitial fibrosis based on the histopathologic analysis of human PKD heart tissue. This tissue remodeling in PKD hearts was associated with increased ECM, perivascular fibrosis, and His-Purkinje fibrosis which could result in an alteration of ventricular properties, disruption of the myocardial contraction (systolic dysfunction), and increased myocardial stiffness (diastolic dysfunction) (Amirrad et al. 2021). Perivascular fibrosis could also disrupt myocardial perfusion, which could lead to myocardial ischemia and worsen the cardiac function (Khan and Sheppard 2006). Furthermore, cardiac fibrosis and His-Purkinje fibrosis could cause inhomogeneous tissue structure, which disrupts electrical impulse propagation and plays a key role in the arrhythmogenicity of PKD hearts (Amirrad et al. 2021, Pala et al. 2019a, b).

TGF-β_1 is a profibrotic cytokine that is generally known as a mediator for the production of extracellular matrix proteins and fibrosis in many different organ systems, including the heart (Khan and Sheppard 2006; Parker et al. 1990; Villarreal and Dillmann 1992). TGF-β_1 is also a key mediator in hypertrophic ventricular remodeling and cardiomyocyte growth (Hanna and Frangogiannis 2019). In our present study, the cardiac TGF-β_1, its receptors, and its downstream signaling pathways in PKD heart samples were evaluated. Our study revealed the overexpression of TGF-β_1 and its receptor in left ventricles which could be the etiology behind the interstitial fibrosis and cardiac hypertrophy.

To study the downstream effect of TGF-β_1, we evaluated phosphorylated Smad3 (pSmad3) and β-catenin expressions in the hearts. It is generally known that increased β-catenin signaling in the cardiac fibroblasts results in increased ECM and cardiac fibrosis (Lin et al. 2017; Ma et al. 2018). Previous studies have also shown that overexpression of β-catenin is sufficient to induce hypertrophic growth in cultured adult myocytes in vitro (Haq et al. 2003) and in vivo (Chen et al. 2006). Our data demonstrated that the expression of the β-catenin in the cardiac myocytes was significantly higher in PKD than non-PKD hearts. Smad3 has a critical role in the fibroblast activation and cardiac fibrosis in response to the TGF-β_1 or pressure overload (Khalil et al. 2017). Our data showed significantly higher expression of pSmad3 in the whole cardiac cells, including cytosol and nucleus, in PKD compared to the non-PKD hearts. This finding suggested TGF-β_1 canonical pathway and pSmad3 as important mediators in fibrotic responses in PKD human hearts.

Along with fibroblast, macrophage infiltration is an additional source of TGF-β_1 production (Kuwahara et al. 2004), and macrophage infiltration has been shown in the fibrotic area in hypertrophic hearts (Hinglais et al. 1994). Our data showed that macrophage M1 and M2 infiltration was significantly higher in PKD heart tissue. This suggested that macrophage M1 and M2 might play crucial roles in cardiac inflammation and, subsequently, myocardial fibrosis in ADPKD.

PKD hearts showed increases collagen I and myofibroblasts. After stress or injury, cardiac fibroblasts transform into myofibroblasts, resulting in increased ECM and α-smooth muscle actin secretion (Francisco et al. 2020; Kong et al. 2014). Consistent with our data, collagen type I synthesis is increased in myocardial fibrosis and results in the cardiac dysfunction (Querejeta et al. 2004). The Hippo-YAP pathway has an important role in modulating cardiomyocyte proliferation and survival (Leach et al. 2017; Lin et al. 2014; Matsuda et al. 2016; Shao et al. 2014). However, recent studies have demonstrated the opposing function of YAP1 in cardiac fibroblast, which can result in cardiac fibrosis (Francisco et al. 2020). Our data indicated that while YAP was increased in PKD myocytes, there was no accumulation of nuclear YAP in PKD. This could probably account for the phosphorylated YAP that retained in the cytoplasm in its inactivated form (Chen et al. 2020).

In summary, our study suggested that hypertrophy and fibrosis occur in human PKD hearts. We report increased TGF-β_1 and its receptor followed by pSmad3 and β-catenin overexpression, which potentially could be the underlying signaling pathway responsible for cardiac abnormality in human PKD (Fig. 7).

Supplementary Material

Refer to Web version on PubMed Central for supplementary material.

Acknowledgements

Jefferey Kim and Delia Tifrea assisted FA and RAE in the procurement and processing of human heart samples at UC Irvine. Denisse Larin-Henriquez assisted FA in reagent preparation and chemical ordering at Chapman University. The authors also acknowledge the support of the Chao Family Comprehensive Cancer Center Experimental Tissue Shared Resource, supported by the National Cancer Institute of the National Institutes of Health under award number P30CA062203.

Funding

This work was supported in part by the NIH HL147311 and HL147311-S1.

References

Amirrad F, Pala R, Shamloo K, Muntean BS, Nauli SM (2021) Arrhythmogenic hearts in PKD2 mutant mice are characterized by cardiac fibrosis, systolic, and diastolic dysfunctions. Front Cardiovasc Med 8

Aranguiz P, Romero P, Vasquez F, Flores-Vergara R, Aravena D, Sanchez G, Gonzalez M, Olmedo I, Pedrozo Z (2021) Polycystin-1 mitigates damage and regulates CTGF expression through AKT activation during cardiac ischemia/reperfusion. Biochim Biophys Acta Mol Basis Dis 1867:165986 [PubMed: 33065236]

Azhar M, Schultz Jel J, Grupp I, Dorn GW 2nd, Meneton P, Molin DG, Gittenberger-de Groot AC, Doetschman T (2003) Transforming growth factor beta in cardiovascular development and function. Cytokine Growth Factor Rev 14:391–407 [PubMed: 12948523]

Balbo BE, Amaral AG, Fonseca JM, de Castro I, Salemi VM, Souza LE, Dos Santos F, Irigoyen MC, Qian F, Chammas R, Onuchic LF (2016) Cardiac dysfunction in Pkd1-deficient mice with phenotype rescue by galectin-3 knockout. Kidney Int 90:580–597 [PubMed: 27475230]

Bujak M, Frangogiannis NG (2007) The role of TGF-beta signaling in myocardial infarction and cardiac remodeling. Cardiovasc Res 74:184–195 [PubMed: 17109837]

Bujak M, Ren G, Kweon HJ, Dobaczewski M, Reddy A, Taffet G, Wang XF, Frangogiannis NG (2007) Essential role of Smad3 in infarct healing and in the pathogenesis of cardiac remodeling. Circulation 116:2127–2138 [PubMed: 17967775]

Chapman AB, Johnson A, Gabow PA, Schrier RW (1990) The renin-angiotensin-aldosterone system and autosomal dominant polycystic kidney disease. N Engl J Med 323:1091–1096 [PubMed: 2215576]

Chapman AB, Johnson AM, Rainguet S, Hossack K, Gabow P, Schrier RW (1997) Left ventricular hypertrophy in autosomal dominant polycystic kidney disease. J Am Soc Nephrol 8:1292–1297 [PubMed: 9259356]

Chebib FT, Hogan MC, El-Zoghby ZM, Irazabal MV, Senum SR, Heyer CM, Madsen CD, Cornec-Le Gall E, Behfar A, Harris PC, Torres VE (2017) Autosomal dominant polycystic kidney patients may be predisposed to various cardiomyopathies. Kidney Int Rep 2:913–923 [PubMed: 29270497]

Chen X, Li Y, Luo J, Hou N (2020) Molecular mechanism of Hippo-YAP1/TAZ pathway in heart development, disease, and regeneration. Front Physiol 11:389 [PubMed: 32390875]

Chen X, Shevtsov SP, Hsich E, Cui L, Haq S, Aronovitz M, Kerkela R, Molkentin JD, Liao R, Salomon RN, Patten R, Force T (2006) The beta-catenin/T-cell factor/lymphocyte enhancer factor signaling pathway is required for normal and stress-induced cardiac hypertrophy. Mol Cell Biol 26:4462–4473 [PubMed: 16738313]

Cnossen WR, Drenth JP (2014) Polycystic liver disease: an overview of pathogenesis, clinical manifestations and management. Orphanet J Rare Dis 9:69 [PubMed: 24886261]

Cornec-Le Gall E, Alam A, Perrone RD (2019) Autosomal dominant polycystic kidney disease. Lancet 393:919–935 [PubMed: 30819518]

Dong K, Zhang C, Tian X, Coman D, Hyder F, Ma M, Somlo S (2021) Renal plasticity revealed through reversal of polycystic kidney disease in mice. Nat Genet 53:1649–1663 [PubMed: 34635846]

Fick GM, Johnson AM, Hammond WS, Gabow PA (1995) Causes of death in autosomal dominant polycystic kidney disease. J Am Soc Nephrol 5:2048–2056 [PubMed: 7579053]

Francisco J, Zhang Y, Jeong JI, Mizushima W, Ikeda S, Ivessa A, Oka S, Zhai P, Tallquist MD, Del Re DP (2020) Blockade of fibroblast YAP attenuates cardiac fibrosis and dysfunction through MRTF-A inhibition. JACC Basic Transl Sci 5:931–945 [PubMed: 33015415]

Frangogiannis NG (2019) The extracellular matrix in ischemic and nonischemic heart failure. Circ Res 125:117–146 [PubMed: 31219741]

Gosse P (2005) Left ventricular hypertrophy as a predictor of cardiovascular risk. J Hypertens Suppl 23:S27–33 [PubMed: 15821448]

Hanna A, Frangogiannis NG (2019) The role of the TGF-beta super-family in myocardial infarction. Front Cardiovasc Med 6:140 [PubMed: 31620450]

Haq S, Michael A, Andreucci M, Bhattacharya K, Dotto P, Walters B, Woodgett J, Kilter H, Force T (2003) Stabilization of beta-catenin by a Wnt-independent mechanism regulates cardiomyocyte growth. Proc Natl Acad Sci U S A 100:4610–4615 [PubMed: 12668767]

Hinglais N, Heudes D, Nicoletti A, Mandet C, Laurent M, Bariety J, Michel JB (1994) Colocalization of myocardial fibrosis and inflammatory cells in rats. Lab Invest 70:286–294 [PubMed: 8139269]

Huang X, Yan L, Kou S, Meng J, Lu Z, Lin CP, Liu C, Zhang H (2021) Generation and characterization of a Myh6-driven Cre knockin mouse line. Transgenic Res 30:821–835 [PubMed: 34542814]

Iglesias CG, Torres VE, Offord KP, Holley KE, Beard CM, Kurland LT (1983) Epidemiology of adult polycystic kidney disease, Olmsted County, Minnesota: 1935–1980. Am J Kidney Dis 2:630–639 [PubMed: 6846334]

Khalil H, Kanisicak O, Prasad V, Correll RN, Fu X, Schips T, Vagnozzi RJ, Liu R, Huynh T, Lee SJ, Karch J, Molkentin JD (2017) Fibroblast-specific TGF-beta-Smad2/3 signaling underlies cardiac fibrosis. J Clin Invest 127:3770–3783 [PubMed: 28891814]

Khan R, Sheppard R (2006) Fibrosis in heart disease: understanding the role of transforming growth factor-beta in cardiomyopathy, valvular disease and arrhythmia. Immunology 118:10–24 [PubMed: 16630019]

Kim K, Drummond I, Ibraghimov-Beskrovnaya O, Klinger K, Arnaout MA (2000) Polycystin 1 is required for the structural integrity of blood vessels. Proc Natl Acad Sci U S A 97:1731–1736 [PubMed: 10677526]

Klein G, Schaefer A, Hilfiker-Kleiner D, Oppermann D, Shukla P, Quint A, Podewski E, Hilfiker A, Schroder F, Leitges M, Drexler H (2005) Increased collagen deposition and diastolic dysfunction but preserved myocardial hypertrophy after pressure overload in mice lacking PKCepsilon. Circ Res 96:748–755 [PubMed: 15761199]

Kong P, Christia P, Frangogiannis NG (2014) The pathogenesis of cardiac fibrosis. Cell Mol Life Sci 71:549–574 [PubMed: 23649149]

Kurschat CE, Muller RU, Franke M, Maintz D, Schermer B, Benzing T (2014) An approach to cystic kidney diseases: the clinician's view. Nat Rev Nephrol 10:687–699 [PubMed: 25266212]

Kuwahara F, Kai H, Tokuda K, Takeya M, Takeshita A, Egashira K, Imaizumi T (2004) Hypertensive myocardial fibrosis and diastolic dysfunction: another model of inflammation? Hypertension 43:739–745 [PubMed: 14967845]

Leach JP, Heallen T, Zhang M, Rahmani M, Morikawa Y, Hill MC, Segura A, Willerson JT, Martin JF (2017) Hippo pathway deficiency reverses systolic heart failure after infarction. Nature 550:260–264 [PubMed: 28976966]

Leier CV, Baker PB, Kilman JW, Wooley CF (1984) Cardiovascular abnormalities associated with adult polycystic kidney disease. Ann Intern Med 100:683–688 [PubMed: 6231874]

Lijnen P, Petrov V (2002) Transforming growth factor-beta 1-induced collagen production in cultures of cardiac fibroblasts is the result of the appearance of myofibroblasts. Methods Find Exp Clin Pharmacol 24:333–344 [PubMed: 12224439]

Lin JC, Kuo WW, Baskaran R, Chen MC, Ho TJ, Chen RJ, Chen YF, Vijaya Padma V, Lay IS, Huang CY (2017) Enhancement of beta-catenin in cardiomyocytes suppresses survival protein expression but promotes apoptosis and fibrosis. Cardiol J 24:195–205 [PubMed: 27734460]

Lin Z, von Gise A, Zhou P, Gu F, Ma Q, Jiang J, Yau AL, Buck JN, Gouin KA, van Gorp PR, Zhou B, Chen J, Seidman JG, Wang DZ, Pu WT (2014) Cardiac-specific YAP activation improves cardiac function and survival in an experimental murine MI model. Circ Res 115:354–363 [PubMed: 24833660]

Ma ZG, Yuan YP, Wu HM, Zhang X, Tang QZ (2018) Cardiac fibrosis: new insights into the pathogenesis. Int J Biol Sci 14:1645–1657 [PubMed: 30416379]

Matsuda T, Zhai P, Sciarretta S, Zhang Y, Jeong JI, Ikeda S, Park J, Hsu CP, Tian B, Pan D, Sadoshima J, Del Re DP (2016) NF2 activates Hippo signaling and promotes ischemia/reperfusion injury in the heart. Circ Res 119:596–606 [PubMed: 27402866]

Morita H (2019) Secondary cardiomyopathy in polycystic kidney disease syndrome. Int Heart J 60:10–11 [PubMed: 30686801]

Nauli SM (2011) An ACE inhibitor improves vascular outcomes in a PKD model. Am J Physiol Renal Physiol 301:F958 [PubMed: 21880832]

Norman J (2011) Fibrosis and progression of autosomal dominant polycystic kidney disease (ADPKD). Biochim Biophys Acta 1812:1327–1336 [PubMed: 21745567]

Ong AC, Ward CJ, Butler RJ, Biddolph S, Bowker C, Torra R, Pei Y, Harris PC (1999) Coordinate expression of the autosomal dominant polycystic kidney disease proteins, polycystin-2 and polycystin-1, in normal and cystic tissue. Am J Pathol 154:1721–1729 [PubMed: 10362797]

Pala R, Mohieldin AM, Shamloo K, Sherpa RT, Kathem SH, Zhou J, Luan Z, Zheng JG, Ahsan A, Nauli SM (2019a) Personalized nanotherapy by specifically targeting cell organelles to improve vascular hypertension. Nano Lett 19:904–914 [PubMed: 30582331]

Pala R, Mohieldin AM, Sherpa RT, Kathem SH, Shamloo K, Luan Z, Zhou J, Zheng JG, Ahsan A, Nauli SM (2019b) Ciliotherapy: remote control of primary cilia movement and function by magnetic nanoparticles. ACS Nano 13:3555–3572 [PubMed: 30860808]

Parker TG, Packer SE, Schneider MD (1990) Peptide growth factors can provoke “fetal” contractile protein gene expression in rat cardiac myocytes. J Clin Invest 85:507–514 [PubMed: 1688886]

Pirson Y, Chauveau D, Torres V (2002) Management of cerebral aneurysms in autosomal dominant polycystic kidney disease. J Am Soc Nephrol 13:269–276 [PubMed: 11752048]

Querejeta R, Lopez B, Gonzalez A, Sanchez E, Larman M, Martinez Ubago JL, Diez J (2004) Increased collagen type I synthesis in patients with heart failure of hypertensive origin: relation to myocardial fibrosis. Circulation 110:1263–1268 [PubMed: 15313958]

Riemann D, Wollert HG, Menschikowski J, Mittenzwei S, Langner J (1994) Immunophenotype of lymphocytes in pericardial fluid from patients with different forms of heart disease. Int Arch Allergy Immunol 104:48–56 [PubMed: 7950405]

Schrier RW (2009) Renal volume, renin-angiotensin-aldosterone system, hypertension, and left ventricular hypertrophy in patients with autosomal dominant polycystic kidney disease. J Am Soc Nephrol 20:1888–1893 [PubMed: 19696226]

Shao D, Zhai P, Del Re DP, Sciarretta S, Yabuta N, Nojima H, Lim DS, Pan D, Sadoshima J (2014) A functional interaction between Hippo-YAP signalling and FoxO1 mediates the oxidative stress response. Nat Commun 5:3315 [PubMed: 24525530]

Suwa Y, Higo S, Nakamoto K, Sera F, Kunimatsu S, Masumura Y, Kanzaki M, Mizote I, Mizuno H, Fujio Y, Hikoso S, Sakata Y (2019) Old-age onset progressive cardiac contractile dysfunction in a patient with polycystic kidney disease harboring a PKD1 frameshift mutation. Int Heart J 60:220–225 [PubMed: 30464138]

Villarreal FJ, Dillmann WH (1992) Cardiac hypertrophy-induced changes in mRNA levels for TGF-beta 1, fibronectin, and collagen. Am J Physiol 262:H1861–1866 [PubMed: 1535758]

Wang Y, Zhang L, Wu GR, Zhou Q, Yue H, Rao LZ, Yuan T, Mo B, Wang FX, Chen LM, Sun F, Song J, Xiong F, Zhang S, Yu Q, Yang P, Xu Y, Zhao J, Zhang H, Xiong W, Wang CY (2021) MBD2 serves as a viable target against pulmonary fibrosis by inhibiting macrophage M2 program. Sci Adv 7

Yu TM, Chuang YW, Yu MC, Huang ST, Chou CY, Lin CL, Chiu CC, Kao CH (2016) New-onset atrial fibrillation is associated with polycystic kidney disease: a nationwide population-based cohort study. Medicine (baltimore) 95:e2623 [PubMed: 26825919]

Zeisberg M, Kalluri R (2013) Cellular mechanisms of tissue fibrosis. 1. Common and organ-specific mechanisms associated with tissue fibrosis. Am J Physiol Cell Physiol 304:C216–225 [PubMed: 23255577]

Significance Statement

- Histopathology analyses of PKD patients' hearts show an increase in extracellular matrix associated with cardiac hypertrophy and fibrosis.
- Hypertrophy- and fibrosis-associated pathways are upregulated in human PKD hearts.
- Human PKD hearts are grossly infiltrated by inflammatory macrophage M1 and M2.

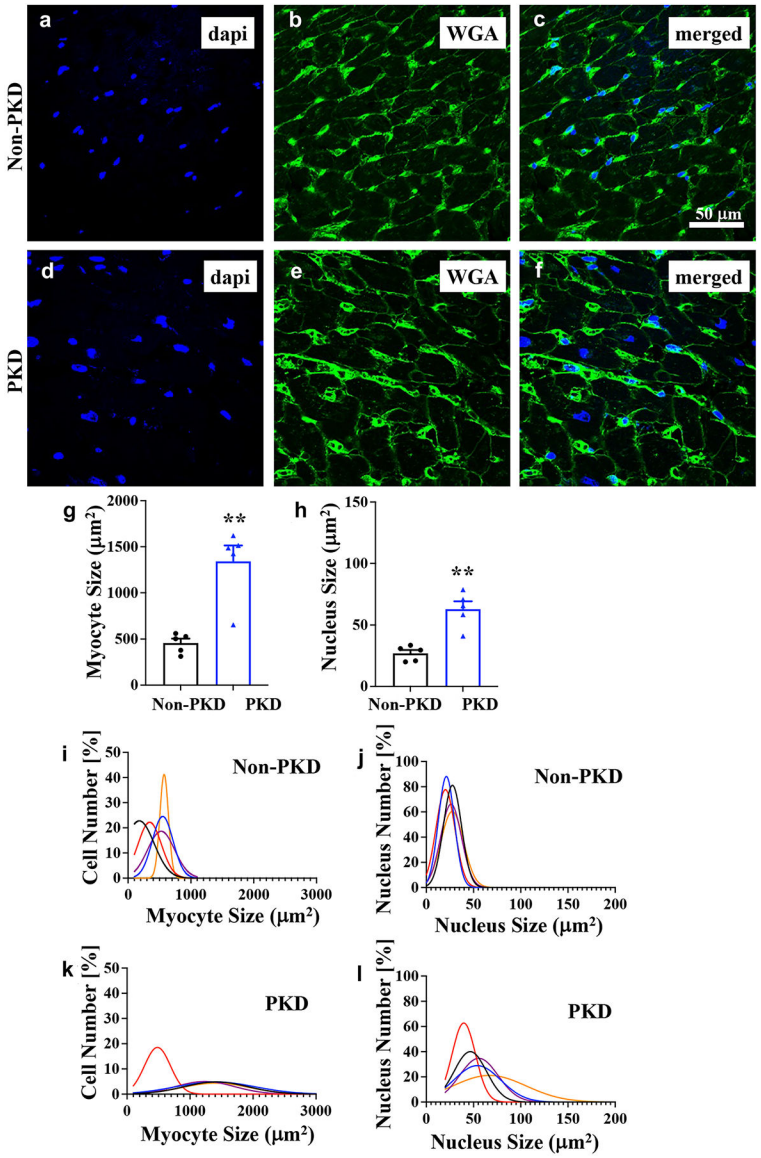

Fig. 1.

Human PKD hearts are characterized by hypertrophy. Cardiac hypertrophy is defined by larger cardiomyocyte overall cell and nucleus size. **a**–**f** Wheat-germ agglutinin (WGA) was used for cell membrane staining to measure myocyte size, and DAPI staining was used to measure nuclear size. Representatives of left ventricle cardiomyocyte hypertrophy and nuclear size are shown. **g**, **h** Myocyte and nuclear size were quantified. **i**, **l** Distribution graph of individual sample from each human heart is shown. $N = 5$ human hearts for each non-PKD and PKD group. $^{**}p < 0.01$

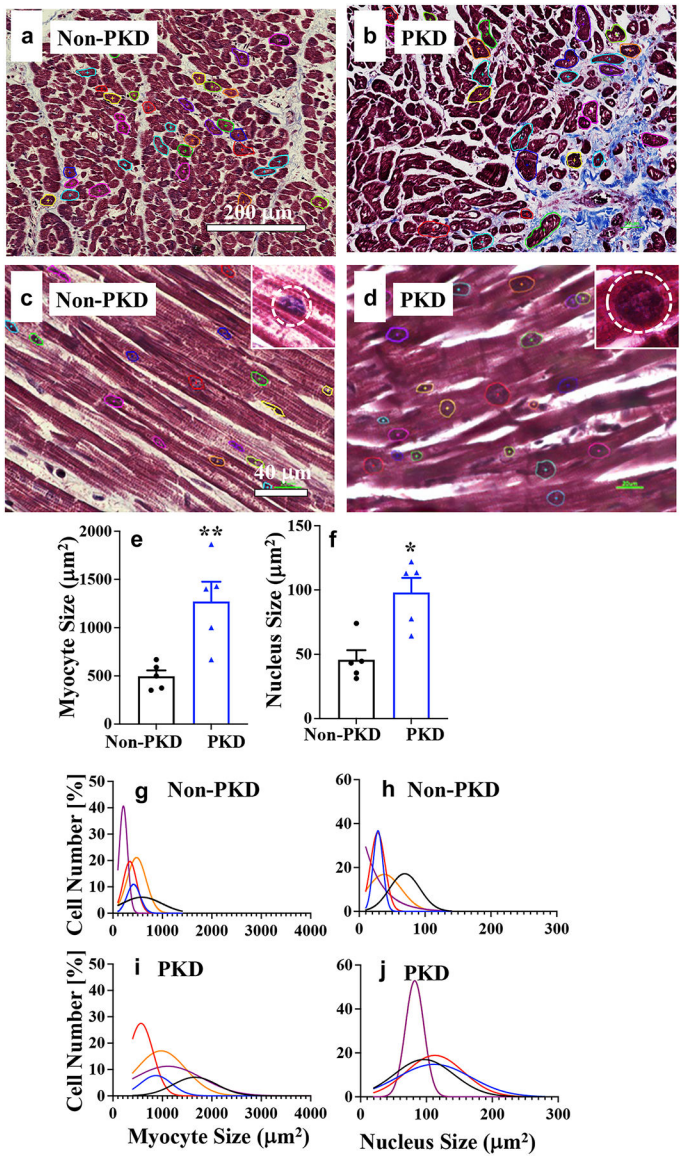

Fig. 2.

The hypertrophy in PKD hearts is characterized by larger myocyte nucleus and overall cell size. **a**–**d** Masson's trichrome stain was performed on non-PKD and PKD human hearts to show cell and nuclear sizes. Color circles represent a random selection of each myocyte and nucleus used for quantitative measurement. The insert shows a representative example of a single nucleus (white circles). **e**, **f** PKD myocytes and nuclei are larger than those of non-PKD. **g**–**j** Distribution graph of individual samples from each human heart is shown. $N = 5$ human hearts for each non-PKD and PKD group. *$p < 0.05$; **$p < 0.01$

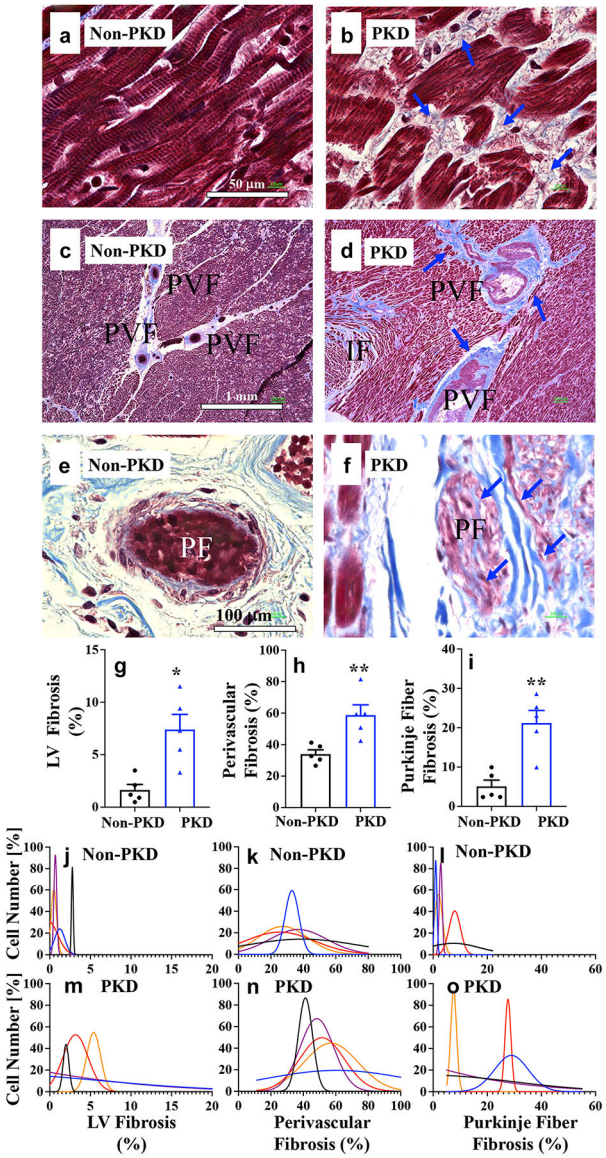

Fig. 3.

Human PKD hearts are characterized by myocardial disorganization and fibrosis. Masson's trichrome stain was performed on non-PKD and PKD human hearts. **a**, **b** Cell organization and matrix surrounding myocytes are shown. PKD hearts are further evidenced to have disorganized myocardial structure and myocyte disarray with increased extracellular matrix and collagen fibers (blue arrows). **c**, **d** PKD hearts are shown to have interstitial fibrosis (IF) and perivascular fibrosis (PVF) as indicated the blue arrows. **e**, **f** Purkinje fibers (PF) in PKD hearts are shown to be fibrotic (arrows). **g**–**i** All quantitative analyses of fibrosis are shown for fibrosis at different parts of the hearts. **j**–**o** Distribution graph of individual samples from each human heart is shown. $N = 5$ human hearts for each non-PKD and PKD group. *$p <$ 0.05; **$p < 0.01$

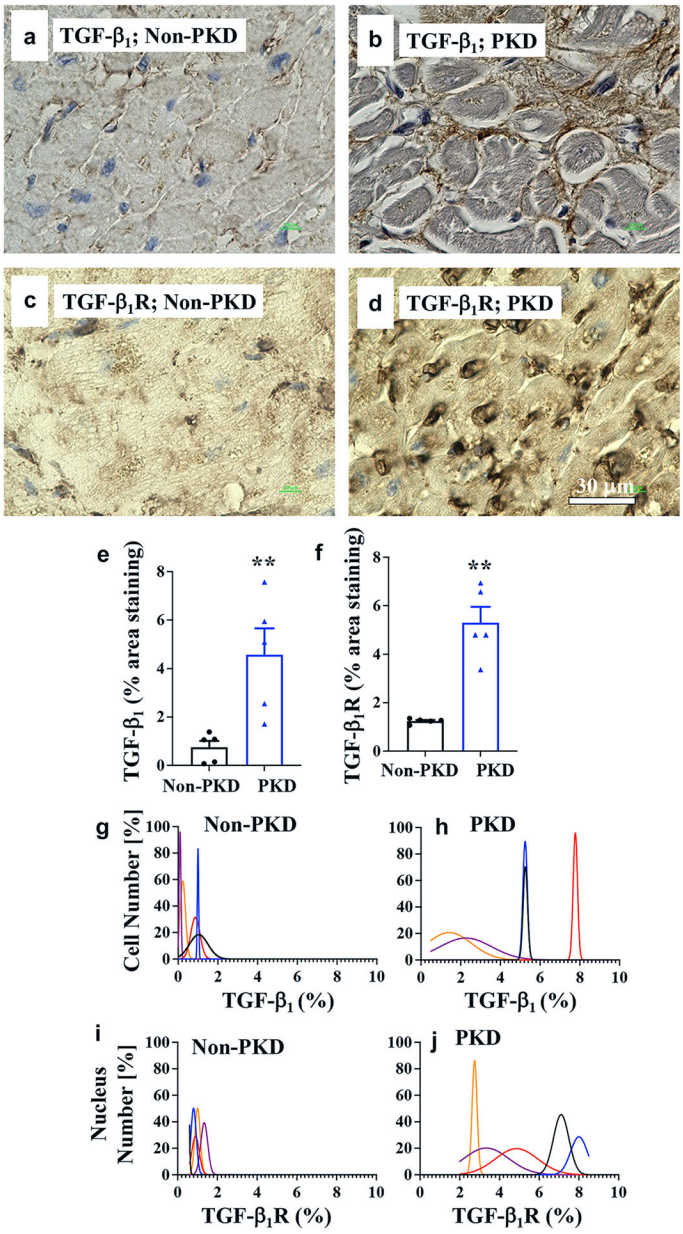

Fig. 4.

Human PKD hearts are characterized by upregulated TGF-β_1 and TGF-β_1 receptor. **a**–**d** Immunohistochemistry staining demonstrated a significant increase of TGF-β_1 and TGF-β_1 receptor. Expression levels of TGF-β_1 and its receptor in non-PKD and PKD heart tissues are indicated by dark-brown color staining. **e**, **f** Quantitative analyses are shown for both TGF-β_1 and TGF-β_1 receptor. **g**–**j** Distribution graph of individual samples from each human heart is shown. $N = 5$ human hearts for each non-PKD and PKD group. $^{**}p < 0.01$

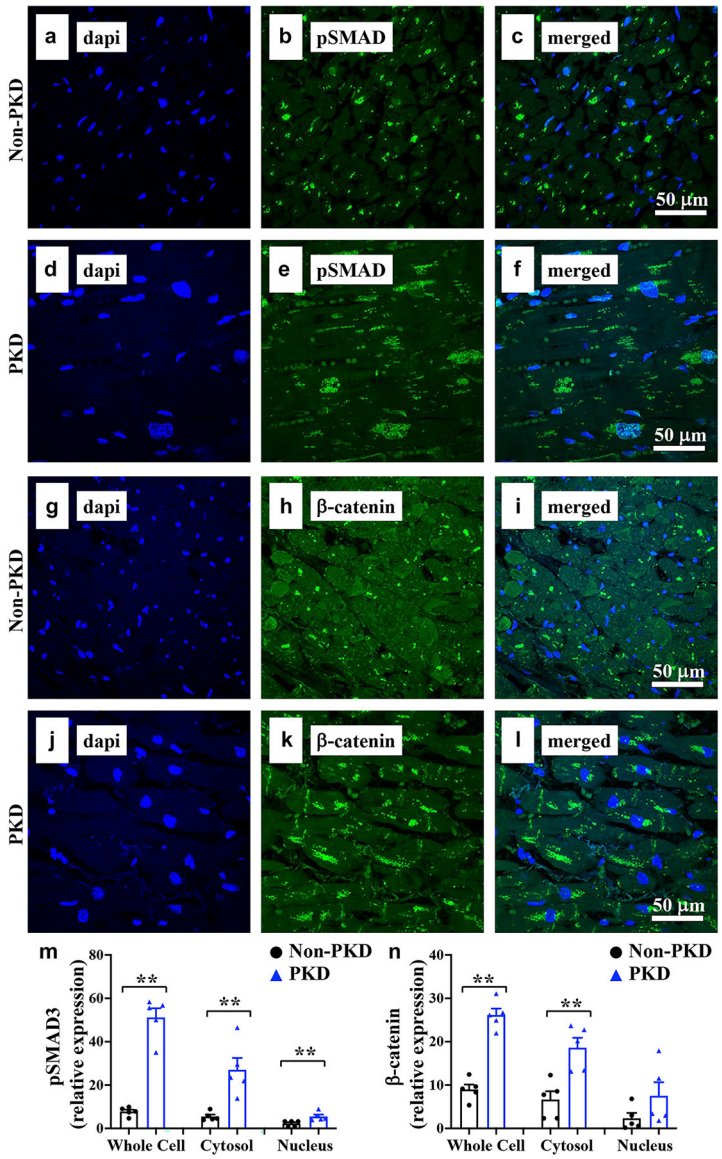

Fig. 5.

Human PKD hearts are characterized by upregulated pSmad3 and β-catenin. **a**–**l** Confocal images were taken to show nucleus (DAPI), pSmad3 expression, and β-catenin expression. The confocal images of nucleus were used to indicate nuclear localization. **m**, **n** Quantitative analyses of pSmad3 and β-catenin are shown for total, cytosolic, and nuclear expressions. *N* = 5 human hearts for each non-PKD and PKD group. $^{**}p < 0.01$

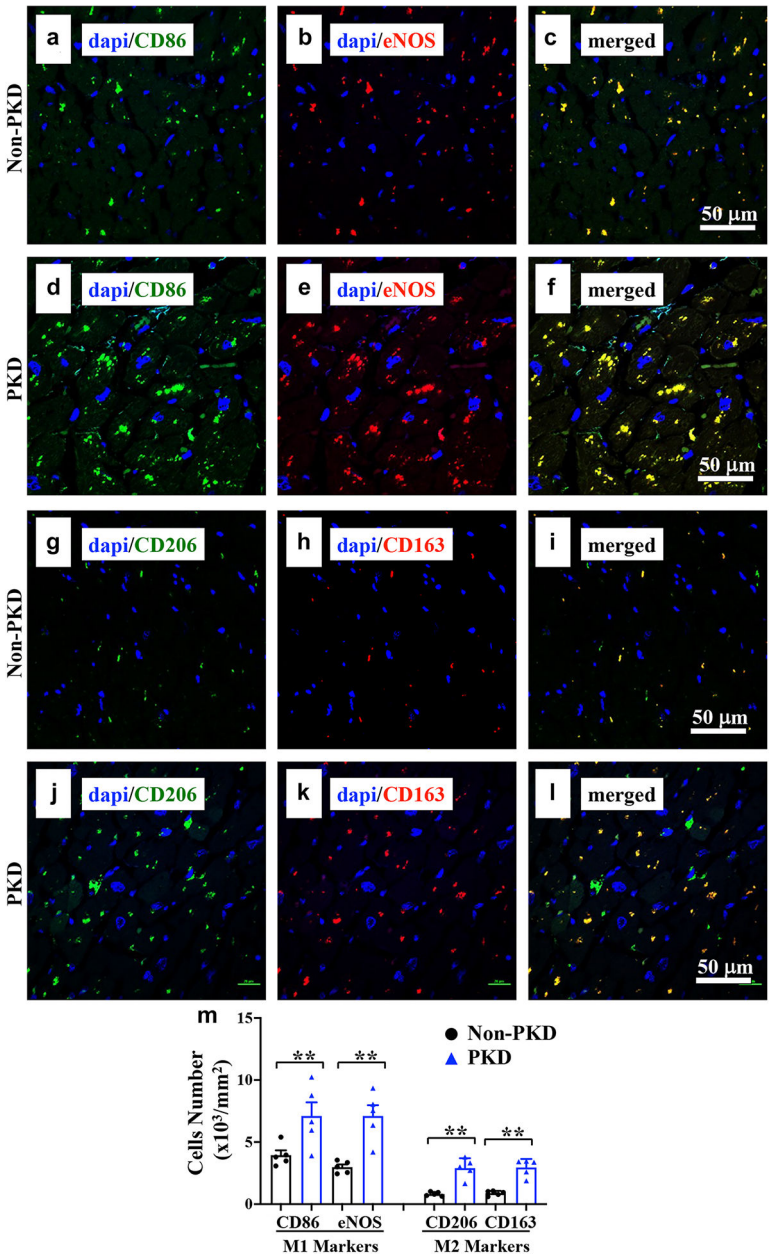

Fig. 6.

Human PKD hearts are infiltrated by macrophages. **a**–**f** Confocal images were taken to show myocyte nucleus (DAPI) with the macrophage M1 markers CD86 and eNOS. **g**–**l** Likewise, confocal images were taken to show myocyte nucleus with the macrophage M2 markers CD206 and CD163. **m** Quantitative analyses of each M1 and M2 marker are shown. $N = 5$ human hearts for each non-PKD and PKD group. $^{**}p < 0.01$

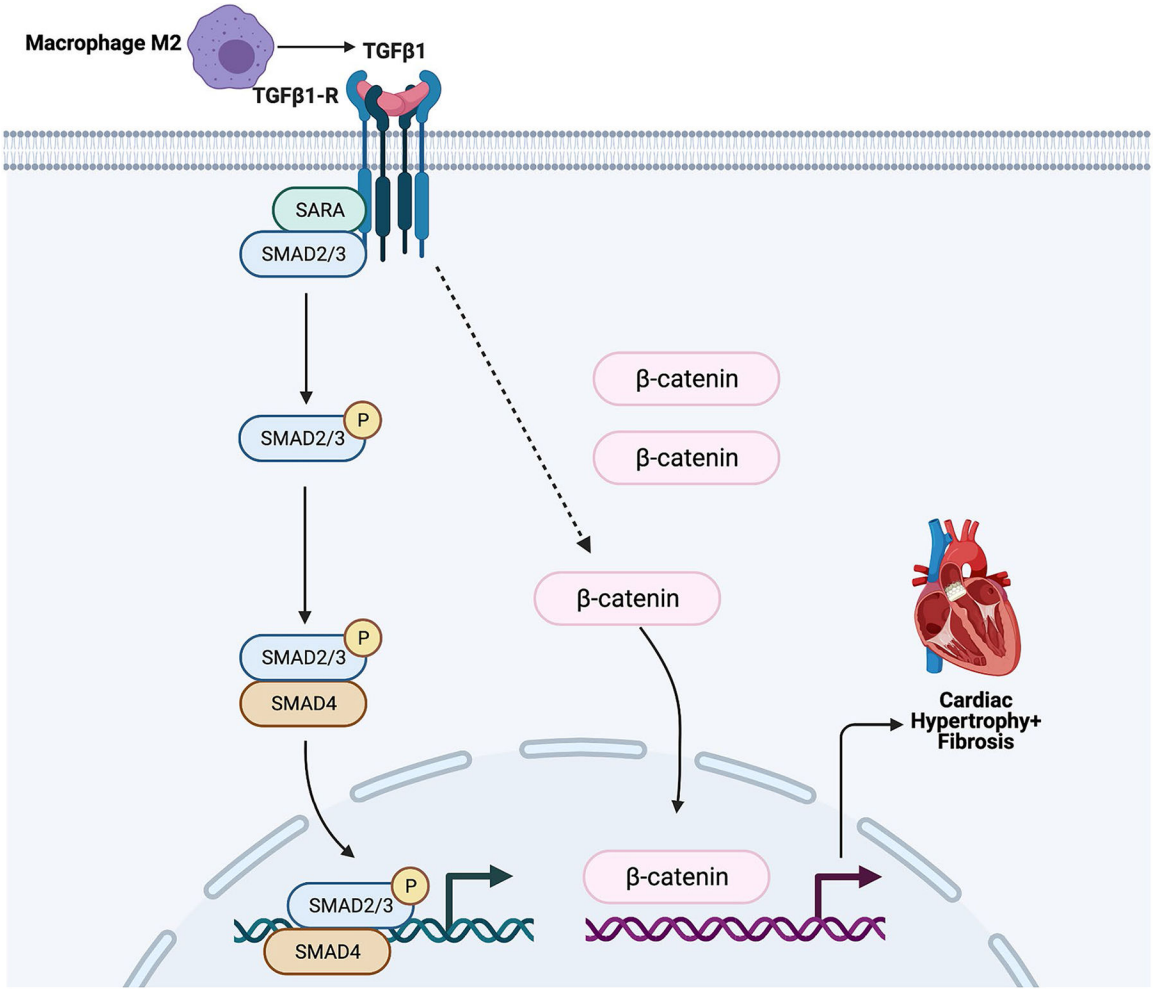

Fig. 7.

Hypothetical diagram summarizing the pathogenesis of human PKD hearts. We hypothesize that hearts from PKD patients are infiltrated by macrophages secreting local TGF-β_1 Subsequent activation of TGF-β_1 receptor results in overexpression of pSMAD3 and β-catenin. Translocation of pSMAD3 and β-catenin to the myocyte nucleus further substantiate the fibrotic pathway activation. The over-expression of TGF-β_1 receptor further exacerbates the activation of fibrotic pathways resulting in hypertrophy characterized by increases in myocyte/nucleus size and perivascular/interstitial fibrosis

Table 1

Characteristics of the five PKD subjects

Gender		Age (years)	Kidney structure	Cause of death	Medical history
Non-PKD	Male	49	Non-cystic	Acute respiratory failure and septic shock	Alcoholic liver disease and cirrhosis
	Male	59	Non-cystic	Postoperative DVT and PE	Gout, asthma, hypersensitivity lung disease, and recurrent glioblastoma
	Male	63	Non-cystic	Metastatic oropharyngeal squamous cell carcinoma/acute pneumonia	Orthostatic hypotension, mild CAD at autopsy
	Male	68	Non-cystic	Aspiration pneumonia	No clinical history; moderate CAD at autopsy
	Male *	79	No abnormality was reported at the time of autopsy	Aspiration pneumonia	Pulmonary hypertension
PKD	Male	50	CKD	Cardiac arrest	3-vessel CABG, aortic valve replacement, congestive heart failure
	Male	54	Transplant kidney autolyzed	DIC, renal failure, cardiopulmonary arrest	Diffuse B-cell lymphoma involving both liver and spleen Extensively, chronic ischemic heart disease
	Male *	55	Right kidney removed; left transplant	Cardiopulmonary failure	Hypertension, metastatic neuroendocrine carcinoma
	Male *	65	2 times kidney transplants	Metastatic renal cell carcinoma from native kidney	Hypertension, LV hypertrophy, mild to moderate CAD, DM type 2, end-stage renal disease
	Male	68	Kidney transplant	Cardiac arrest, acute myocardial infarction	Moderate to severe coronary atherosclerosis, end-stage renal disease

CAD Coronary Artery Disease, **CKD** Chronic Kidney disease, **DIC** Disseminated Intravascular Coagulation, **DM** Diabetes Mellitus, **DVT** Deep Venous Thrombosis, **ESRF** End-stage Renal Failure, **PE** Pulmonary Edema

* Hypertension